Contrib. Astron. Obs. Skalnaté Pleso **36**, 26 – 46, (2006)

The photometric study of the symbiotic binary YY Her

I. The eclipsing model

L. Hric[1], R. Gális[2], P. Niarchos[3], A. Dobrotka[4], V. Šimon[5], L. Šmelcer[6], Z. Velič[7], P. Hájek[8], K. Gazeas[3], P. Sobotka[9] and K. Koss[8]

[1] *Astronomical Institute of the Slovak Academy of Sciences 059 60 Tatranská Lomnica, The Slovak Republic, (E-mail: hric@ta3.sk)*

[2] *Faculty of Sciences, University of P. J. Šafárik, Moyzesova 16, 041 54 Košice, The Slovak Republic, (E-mail: galis@kosice.upjs.sk)*

[3] *Department of Astrophysics, Astronomy and Mechanics, University of Athens, GR 157 84 Zografos, Athens, Greece, (E-mail: pniarcho@uoa.gr)*

[4] *Faculty of Materials Science and Technology STU, 917 24 Trnava, The Slovak Republic, (E-mail: dobrotka@mtf.stuba.sk)*

[5] *Astronomical Institute of the Academy of Sciences of the Czech Republic, 251 65 Ondřejov, The Czech Republic (E-mail: simon@asu.cas.cz)*

[6] *Public Observatory, 757 01 Valašské Meziříčí, The Czech Republic (E-mail: lsmelcer@astrovm.cz)*

[7] *Private Observatory, 018 61 Beluša, The Slovak Republic (E-mail: osbdpb@px.psg.sk)*

[8] *Public Observatory, 682 01 Vyškov, The Czech Republic*

[9] *MEDUZA Group, 616 01 Brno, The Czech Republic*

Received: April 15, 2005; Accepted: November 9, 2005

Abstract. The extensive long-term CCD and photoelectric photometric observations of the classical symbiotic star YY Her covering the period of its post-outburst activity (JD 2 451 823 – 2 452 996) are presented. We explain the periodic variations of the brightness of YY Her by the eclipses of the components in the symbiotic system. The model with a deformed (non-homogeneous) envelope, surrounding the white dwarf is discussed. In addition, we observed a flare in about JD 2 452 440, during the primary minimum, that was later followed by an energetic outburst in JD 2 452 700.

Key words: stars: binaries: symbiotic – stars: individual: YY Her

1. Introduction

YY Her belongs to the classical symbiotic binaries with nova-like outbursts. It was discovered to be a variable by Wolf (1919). On the basis of the next observations (Plaut, 1932 and Böhme, 1938), it has been classified as an irregular variable. Finally, Herbig (1950) described the spectrum in detail and identified it as symbiotic. In his observations, the star exhibited a strong emission spectrum superimposed on the late-type absorption one with strong TiO bands corresponding to a type of about M2. The emission lines were due to the hydrogen lines H_β, H_γ, H_δ and He II as well as [O III]. Michalitsianos *et al.* (1982) published the IUE ultraviolet observations of YY Her and recognised that the system showed very strong high-excitation emission lines, which is in contradiction with the result obtained by Allen (1979) from the optical observations. It is possible to explain this conflict in terms of changes in the thermal excitation over some time scales.

The spectroscopic observations of YY Her in the optical region have been performed by Blair *et al.* (1983). The spectrum shows many of the same characteristics as described by Herbig (1950). Synthetic spectra for many symbiotic stars were computed by Kenyon & Webbink (1984). They used three-source model: a late-type giant, a hot companion and a surrounding nebula that is photo-ionised by the hot component. Their analysis gave a satisfactory fit for the main sequence (MS) star as an accretor with $\mathrm{d}M/\mathrm{d}t \approx 1.6 \times 10^{-5}$ $\mathrm{M}_\odot$ yr^{-1}. They deduced the reddening for this model to be $E_{\mathrm{B-V}} = 0.13 \pm 0.04$ mag. Huang (1984) reported an optical spectroscopic observation with a rather low dispersion of 3.9 nm mm^{-1} and found the spectral type G8Iab for the cool component. It is worth noting that the observations were obtained during the primary minimum.

Nussbaumer *et al.* (1988) studied C, N, O abundances in 24 symbiotic stars from the IUE UV data. They found that symbiotic nebulae have the CNO composition very similar to those of the M giants. The hot components of 21 symbiotic stars were investigated by means of continua and He II lines of the IUE spectra by Mürset *et al.* (1991). For the hot component of YY Her they obtained a temperature of 100 000 K and a luminosity of 1100 $L_\odot$. Munari *et al.* (1997 a) investigated the spectroscopic and photometric behaviour of YY Her during the quiescence as well as during the outburst in 1993. They determined the physical and geometrical parameters as follows: for the cool giant filling its Roche lobe $T_\mathrm{c} = 3500$ K, $L_\mathrm{c} \approx 3600$ $L_\odot$, $\sum M = 2$ $M_\odot$, $q = M_\mathrm{c}/M_\mathrm{h} = 2$; for the hot component $L_{\mathrm{h,min}} = 2000$ $L_\odot$, $L_{\mathrm{h,max}} = 15000$ $L_\odot$ and the temperature of the white dwarf decrease from 110 000 K to 82 000 K during outburst.

YY Her is a little bit fainter than most of the monitored symbiotic stars, this is the reason that the historical light curve has been covered insufficiently and inhomogeneously so far. The photometric history has been described by Munari *et al.* (1997 b). 4 large outbursts (1914–1918, 1930–1933, 1981–1982, 1993–1996) and 6 small eruptions in 1890, 1903, 1942, 1954, 1965 and 1974 were

observed. The last large outburst that appeared in 1993 was studied in detail by Tatarnikova *et al.* (2000). They suggested from the duration of the eclipse in 1997 that the cool component of YY Her fills its Roche lobe. The bulk of the envelope's volume emission measure is concentrated around the hot component in a region with rather sharp boundaries ($r < R_c$) and the line of sight is close to the binary's orbital plane. Munari *et al.* (1997 a) and Munari *et al.* (1997 b) analysed all the available photometric and spectroscopic data and concluded that eclipses should be excluded as the cause of the light variability.

Hric *et al.* (2001 a) published a long-term CCD photometric monitoring of the YY Her system. They discovered that except the primary minima, secondary minima were also present in the light curves, and they proposed to explain the photometric behaviour of the system in terms of eclipses. The presence of the secondary minimum was, however, indicated only by three photometric observations from one observatory. This uncertainty stimulated us to activate an international photometric campaign for a detailed coverage of the light curve during the period of the expected secondary minimum.

Tatarnikova *et al.* (2001) explained the observation of the minimum by the model with the cool component filling much of its Roche lobe and having a hot spot on the hemisphere facing the hot component. Mikolajewska *et al.*(2002) explained the light variability of YY Her by a combination of the ellipsoidal changes and sinusoidal variations of the nebular continuum and line emission. Recently, Waagen (2003) reported the first outburst of YY Her since May 1993.

2. Observations

The photometric observational material used in this work was taken from two basic sources. On the basis of the previous knowledge about the studied object, we included the star into the long-term photometric monitoring that was realised at the Beluša Observatory, Slovakia (Be) (The Newton telescope 180/700 mm, home-made CCD (TC211 chip) + $BVRI$ (Kron-Cousins)) from 1995. The observations taken here in the period of JD 2 449 899 – 2 451 817 led to the discovery of the secondary minimum in YY Her and were published by Hric *et al.* (2001 a).

The second source of the observations comes from the two international campaigns we coordinated in 2001 - 2003 (Hric *et al.* 2001 b). These campaigns were oriented to confirm the presence of the secondary minimum as well as to the detailed covering of both minima. The following observatories and equipments, except (Be), were integrated to this campaign:
- University of Athens, Greece (At) (0.4 m reflector f/8, CCD SBIG ST-8, $BVRI$ (Bessell)),
- the Kryonerion Observatory, Greece (Kr) (1.2 m Cassegrain, PPM, UBV (Johnson)),
- the Valašské Meziříčí Observatory, Czech Republic (VM) (Schmidt-Cassegrain 280/1765 mm, CCD ST-7, VR (Kron-Cousins)),

- the Vyškov Observatory, The Czech Republic (Vy) (RL 300/1200 mm, CCD ST-7, $BVRI$ (Bessell)),
- N. Copernicus Observatory, Brno, The Czech Republic, (Br) (Nasmyth 400/1200 mm, CCD ST-7, $BVRI$ (Kron-Cousins)),
- Astronomical Institute, Academy of Sciences, Ondřejov, Czech Republic (On) (Maksutov 180/1000 mm, CCD SBIG ST-6, VRI (Kron-Cousins)),
- Stará Lesná Observatory of the Astronomical Institute, Slovakia, (SL) (0.6 m Cassegrain, PPM, $UBVR$ (Johnson)).

In this campaign a total of 217, 463, 323 and 290 observational data in the B, V, R and I filter, respectively, were obtained covering the interval of JD 2 451 823 – 2 452 996. We have finished the campaign to the end of the season 2003. The campaign fulfilled its aim very well and actually exceeded our expectations, since not only the whole orbital cycle was covered, but two flares were also detected in the primary minimum that were followed by an outburst (JD 2 452 694) maximum which was observed also photoelectrically. This unexpected activity deformed the shape of the primary minimum and made difficult the detailed analysis of the light curves. On the other side this is the unique possibility to study the energetic balance and the relations of the events before and during the outburst. The daily averages from the obtained data for the individual observatories were calculated. The values of Julian dates were computed as the average values from the individual observations in various filters. All the data are listed in Table 1 which contains the Modified Julian Date (MJD), the original observations in the B, V, R and I pass-bands as well as the abbreviation of the observatory (Ob).

Our new data (described above) were supplemented by the older data secured in the framework of the international campaign of long-term monitoring of symbiotic stars (Hric & Skopal, 1989) at the Kryonerion, Skalnaté Pleso and Wroclaw observatories. Moreover, the UBV photoelectric photometry published by Munari et al. (1997 a, b), Tatarnikova et al. (2000) and Mikolajewska (2002) as well as IR photoelectric photometry by Munari et al. (1997 b) were adopted.

3. Data reduction

During the preparation of the campaign, we attempted to choose such equipment and detectors that would enable us to obtain a homogeneous set of observations. Although mainly the CCD equipment was preferred because of a better connection to the international system, the equipments using the photoelectric photometry were also included (Kr, SL). Despite a careful approach, we were not successful in obtaining the complete homogeneous sets of the observations and it was necessary to correct the individual observations from different observatories. To obtain the applicable homogeneous sets, the observations from the individual observatories were analysed in detail in order to find the zero levels. In addition, concerning the fact that we wanted to study also the historical

Table 1. Photometry of YY Her in the B, V, R and I filters

MJD	B	V	R	I	Ob	MJD	B	V	R	I	Ob
49899.410	-	12.42	11.43	10.34	Be	51878.207	14.20	13.28	11.97	10.62	Be
49935.371	-	12.43	11.43	10.36	Be	51952.636	13.97	12.96	11.78	10.52	Be
49979.346	-	12.48	11.47	10.35	Be	51955.662	-	13.03	11.80	10.47	Br
50000.307	-	12.75	11.59	10.37	Be	51957.661	-	13.02	11.78	10.48	Br
50012.317	-	12.78	11.63	10.42	Be	51983.617	-	12.90	11.69	10.42	Br
50515.608	13.70	12.72	11.59	10.42	Be	51984.665	14.22	13.03	11.88	10.46	At
50579.419	13.94	12.78	11.61	10.42	Be	51996.559	14.17	13.01	11.86	10.45	At
50604.380	13.99	12.78	11.66	10.45	Be	52001.524	13.86	12.90	11.68	10.46	Be
50611.435	14.11	12.86	11.67	10.44	Be	52003.582	14.25	12.98	11.83	10.43	At
50639.399	14.36	13.12	11.86	10.54	Be	52004.585	14.11	12.97	11.83	10.44	At
50641.398	14.26	13.04	11.84	10.50	Be	52005.616	-	12.90	11.69	10.44	Br
50658.369	14.20	13.07	11.93	10.57	Be	52024.571	-	12.81	11.60	10.41	Br
50672.357	14.31	13.22	11.99	10.63	Be	52024.608	14.09	12.87	11.75	10.41	At
50693.316	14.34	13.35	12.02	10.65	Be	52027.441	14.08	12.90	11.74	10.42	At
50708.293	14.70	13.37	12.07	10.65	Be	52031.448	14.05	12.75	11.58	10.46	Be
50720.309	14.41	13.24	12.00	10.62	Be	52032.610	14.16	12.85	11.72	10.41	At
50745.249	14.04	13.13	11.86	10.50	Be	52040.403	13.99	12.87	11.73	10.47	Vy
50750.248	14.23	13.03	11.82	10.50	Be	52040.466	-	12.79	11.60	10.42	Br
50773.205	14.05	13.00	11.78	10.49	Be	52041.396	14.12	12.87	11.76	10.48	Vy
50937.430	13.76	12.72	11.52	10.49	Be	52042.410	13.96	12.86	11.73	10.47	Vy
50942.451	-	12.77	11.52	10.48	Be	52043.393	14.00	12.88	11.75	10.47	Vy
50972.402	13.81	12.84	11.63	10.57	Be	52043.444	13.94	12.75	11.60	10.47	Be
50986.393	13.98	12.88	11.65	10.59	Be	52044.356	13.95	12.85	11.71	10.47	Vy
50998.441	13.89	12.92	11.67	10.60	Be	52045.500	14.04	12.87	11.75	10.39	At
51028.393	13.68	12.64	11.51	10.44	Be	52047.455	14.01	12.87	11.73	10.46	Vy
51066.304	13.82	12.65	11.48	10.42	Be	52049.416	13.94	12.80	11.60	10.47	Be
51080.293	13.79	12.69	11.49	10.42	Be	52049.541	13.52	12.83	11.62	10.43	Br
51123.244	13.98	12.80	11.60	10.44	Be	52052.543	13.51	12.82	11.62	10.43	Br
51130.241	13.81	12.89	11.65	10.44	Be	52053.372	14.11	12.88	11.75	10.47	Vy
51250.591	14.46	13.37	12.02	10.65	Be	52054.386	14.07	12.86	11.72	10.48	Vy
51277.523	14.39	13.35	12.10	10.68	Be	52054.532	-	12.83	11.62	10.44	Br
51299.413	-	-	-	10.64	Be	52055.402	14.03	12.87	11.73	10.48	Vy
51304.432	13.99	13.33	12.01	10.64	Be	52058.346	14.07	12.83	11.69	10.42	At
51308.528	-	13.40	-	-	Br	52059.518	13.51	12.77	11.56	10.40	Br
51317.407	14.44	13.19	11.88	10.53	Be	52060.416	13.97	12.82	11.69	10.47	Vy
51317.471	-	13.40	-	-	Br	52061.354	14.02	12.84	-	10.41	At
51320.474	-	13.40	-	-	Br	52073.532	13.49	12.81	11.61	10.45	Br
51323.390	14.20	13.10	11.86	10.53	Be	52074.379	13.87	12.86	11.69	10.48	Vy
51355.396	13.93	12.96	11.78	10.48	Be	52075.427	-	12.76	11.56	10.46	On
51356.394	13.94	12.94	11.76	10.46	Be	52075.512	-	12.82	11.60	10.43	Br
51363.390	14.12	12.91	11.72	10.45	Be	52076.364	13.98	12.85	11.70	10.48	Vy
51394.377	14.20	12.91	11.69	10.46	Be	52081.470	-	12.80	11.57	10.48	On
51471.310	13.91	12.71	11.55	10.43	Be	52083.322	14.00	12.93	11.73	-	At
51616.600	13.81	12.87	11.62	10.52	Be	52083.406	14.00	12.86	11.72	10.50	Vy
51643.531	13.83	12.75	11.56	10.48	Be	52084.323	14.03	12.90	11.72	10.46	At
51657.458	13.92	12.83	11.62	10.49	Be	52085.320	14.10	12.89	11.72	-	At
51665.453	13.81	12.80	11.56	10.45	Be	52086.311	14.15	12.91	11.72	10.46	At
51698.423	14.08	12.83	11.67	10.48	Be	52086.399	13.94	12.88	11.71	10.50	Vy
51705.419	13.82	12.79	11.60	10.44	Be	52086.440	-	12.81	11.58	10.49	On
51717.420	14.27	12.91	11.69	10.49	Be	52087.327	14.04	12.90	11.71	-	At
51731.422	14.13	12.84	11.69	10.50	Be	52087.397	14.03	12.77	11.58	10.49	Be
51751.437	13.99	12.86	11.69	10.48	Be	52087.409	-	12.91	-	-	VM
51767.362	13.94	12.95	11.75	10.51	Be	52088.321	14.21	12.99	11.74	-	At
51778.347	14.17	12.99	11.76	10.51	Be	52088.424	13.51	12.83	11.60	10.46	Br
51797.303	14.14	12.93	11.75	10.50	Be	52089.317	-	12.83	11.76	-	At
51815.275	14.26	13.21	11.97	10.61	Be	52090.313	14.25	12.86	11.73	-	At
51817.276	14.18	13.24	11.97	10.62	Be	52090.487	13.98	12.86	11.71	10.50	Vy
51823.291	13.81	13.14	11.89	10.58	Be	52091.320	14.01	12.88	11.73	-	At
51833.295	14.15	13.17	11.92	10.61	Be	52091.387	14.00	12.85	11.72	10.49	Vy
51839.252	14.31	13.29	12.01	10.64	Be	52091.401	-	12.93	-	-	VM
51854.244	14.35	13.49	12.12	10.72	Be	52092.326	14.14	12.92	11.70	-	At

Table 1. Photometry of YY Her in the B, V, R and I filters - continued

MJD	B	V	R	I	Ob	MJD	B	V	R	I	Ob
52093.505	-	12.25	-	-	Br	52152.322	13.91	13.09	11.83	10.71	Be
52094.342	14.01	12.95	11.75	-	At	52152.328	-	13.22	-	-	VM
52095.354	-	12.87	-	-	VM	52155.316	-	13.10	11.77	10.69	Be
52095.390	13.95	12.86	11.74	10.51	Vy	52155.367	-	13.14	-	-	VM
52096.385	13.97	12.88	11.71	10.51	Vy	52156.346	-	13.19	-	-	VM
52096.416	-	12.89	-	-	VM	52159.433	14.24	13.11	11.86	10.66	At
52097.413	-	12.89	-	-	VM	52160.319	14.00	12.98	11.75	10.66	Be
52099.377	13.99	12.90	11.74	-	At	52164.373	14.09	13.09	11.87	10.62	At
52101.404	-	12.94	-	-	VM	52165.396	14.15	13.13	-	-	Kr
52103.320	14.12	12.98	11.79	10.53	At	52169.337	14.10	13.07	-	-	Kr
52103.412	-	12.39	-	-	Br	52171.296	14.15	13.07	11.85	10.60	At
52103.442	-	12.98	11.77	-	VM	52172.289	14.00	12.94	11.69	10.62	Be
52105.363	13.94	12.96	11.82	10.57	Vy	52172.310	-	13.01	-	-	VM
52105.405	-	13.00	-	-	VM	52173.288	13.98	12.93	11.68	10.60	Be
52106.358	14.03	-	-	10.58	Vy	52173.302	-	13.06	-	-	VM
52107.322	14.09	13.04	11.89	-	At	52174.330	13.91	-	-	10.61	Vy
52112.445	-	12.45	-	-	Br	52174.355	-	13.04	-	-	VM
52116.321	14.21	13.12	11.91	10.59	At	52176.233	14.02	13.01	11.81	10.56	At
52116.384	14.40	13.05	11.94	10.63	Vy	52185.232	-	12.91	11.61	10.51	Br
52118.368	14.32	13.10	11.95	10.68	Vy	52185.288	-	12.99	-	-	VM
52118.473	-	13.12	-	-	VM	52186.279	-	12.98	-	-	VM
52119.349	14.05	13.11	11.94	10.68	Vy	52186.281	14.03	13.01	11.75	10.55	At
52119.400	-	13.10	11.72	10.66	On	52186.286	-	12.96	11.61	10.49	Br
52121.340	14.42	13.14	11.96	10.68	Vy	52187.312	-	12.82	11.57	10.50	Br
52121.398	14.15	13.03	11.80	10.67	Be	52188.252	-	-	-	10.55	Vy
52122.350	-	13.09	11.80	10.62	Br	52188.284	-	12.99	-	-	VM
52122.364	14.15	13.13	11.94	10.69	Vy	52191.267	-	12.95	-	-	VM
52123.346	14.12	13.15	11.88	-	Vy	52192.261	14.01	12.93	11.72	10.51	At
52123.495	-	13.16	-	-	VM	52193.300	-	12.82	11.57	10.52	On
52124.335	14.17	13.15	11.94	10.70	Vy	52193.309	-	12.94	-	-	VM
52124.374	-	13.09	11.83	10.66	Br	52194.261	-	12.86	11.60	10.51	Br
52127.432	14.23	13.13	11.97	10.72	Vy	52195.225	13.97	-	-	10.55	Vy
52128.331	14.38	13.20	11.97	10.73	Vy	52195.284	-	12.84	11.57	10.48	Br
52129.336	14.33	13.20	11.98	10.73	Vy	52196.233	13.81	-	-	10.53	Vy
52129.343	-	13.15	11.86	10.67	Br	52196.300	-	12.81	11.58	10.54	On
52131.327	14.15	-	-	10.73	Vy	52197.228	13.76	-	-	10.53	Vy
52131.378	-	13.23	11.82	-	VM	52198.243	-	12.91	-	-	VM
52133.331	14.27	-	-	10.74	Vy	52201.229	-	12.88	-	-	VM
52133.407	-	13.26	11.89	-	VM	52206.230	13.97	12.86	11.69	10.47	At
52134.352	-	13.25	-	-	VM	52214.221	-	12.89	-	-	VM
52134.363	-	13.18	11.82	10.76	On	52215.275	-	12.83	-	-	VM
52134.371	14.11	13.11	11.87	10.72	Be	52218.280	-	12.84	-	-	VM
52136.382	-	13.26	11.84	-	VM	52219.279	-	12.85	-	-	VM
52136.393	-	13.11	11.73	10.74	On	52224.311	-	11.84	11.48	10.40	Br
52137.370	-	13.12	11.85	10.73	On	52229.205	-	12.82	-	-	VM
52137.387	-	13.26	-	-	VM	52229.227	14.05	12.86	-	10.48	Vy
52138.367	-	13.13	11.83	10.70	Br	52231.203	13.97	12.87	-	10.47	Vy
52138.378	-	13.27	11.85	-	VM	52231.226	-	12.82	-	-	VM
52139.328	14.03	-	-	10.75	Vy	52253.195	-	12.87	-	-	VM
52139.348	-	13.24	-	-	VM	52321.625	13.97	12.88	-	10.43	Vy
52146.336	-	13.28	-	-	VM	52322.647	14.26	12.88	-	10.43	Vy
52146.340	-	13.30	11.95	10.66	On	52344.554	-	12.96	-	-	VM
52146.398	14.10	-	-	10.75	Vy	52345.569	14.00	12.80	11.64	10.43	Be
52147.340	-	13.25	11.90	10.62	On	52352.542	-	12.93	-	-	VM
52147.348	-	13.29	-	-	VM	52363.521	14.09	12.95	11.73	10.52	Be
52148.324	14.10	13.10	11.83	10.71	Be	52363.525	14.09	13.03	-	10.54	Vy
52148.470	-	-	11.86	-	On	52363.570	-	13.00	11.75	10.45	Br
52149.379	-	13.16	11.85	10.68	Br	52364.506	14.13	13.06	-	10.53	Vy
52149.445	14.22	13.26	11.93	10.70	At	52364.506	-	13.02	-	-	VM
52150.315	-	13.17	11.89	10.70	Br	52369.548	14.18	13.07	-	10.54	Vy
52151.378	-	13.22	-	-	VM	52370.584	-	13.05	11.77	10.49	Br

Table 1. Photometry of YY Her in the B, V, R and I filters - continued

MJD	B	V	R	I	Ob	MJD	B	V	R	I	Ob
52386.515	-	13.24	11.91	10.53	Br	52457.383	-	13.41	-	-	VM
52389.401	-	13.23	11.92	10.56	Br	52457.425	14.47	13.30	12.03	10.64	Be
52395.433	-	13.33	12.01	10.59	Br	52459.371	-	13.44	-	-	VM
52395.442	14.30	13.30	12.04	10.65	Be	52459.390	14.77	13.42	12.16	10.66	Vy
52396.437	-	13.40	-	-	VM	52460.373	14.66	13.44	12.17	10.66	Vy
52398.497	-	13.35	12.00	10.69	On	52460.388	-	13.45	-	-	VM
52402.435	-	13.47	-	-	VM	52461.360	14.72	13.48	12.18	10.66	Vy
52402.443	-	13.36	12.04	10.63	Br	52461.394	-	13.41	12.06	10.62	Br
52403.442	-	13.45	-	-	VM	52461.414	-	13.44	-	-	VM
52404.430	14.52	13.49	-	10.72	Vy	52461.436	-	13.31	12.01	10.67	On
52404.440	-	13.46	-	-	VM	52464.405	14.50	13.37	12.07	10.65	Be
52404.481	-	13.40	12.04	10.71	On	52464.409	-	13.44	-	-	VM
52410.425	14.47	13.39	12.11	10.72	Be	52465.419	-	13.28	12.01	10.66	On
52410.474	-	13.51	-	-	VM	52465.426	-	13.47	-	-	VM
52411.449	-	13.54	-	-	VM	52466.381	-	13.47	-	-	VM
52411.453	-	13.46	12.08	10.73	On	52467.429	-	13.46	-	-	VM
52412.410	14.67	13.49	-	10.75	Vy	52468.384	14.59	13.45	12.17	10.67	Vy
52413.334	14.39	13.45	-	10.72	Vy	52473.461	-	13.38	-	-	VM
52413.351	-	13.43	12.09	10.68	Br	52478.329	-	13.25	11.95	10.55	Br
52413.426	14.40	13.41	12.13	10.72	Be	52483.339	14.45	13.25	12.04	10.55	Vy
52417.437	-	13.59	-	-	VM	52483.340	-	13.14	11.91	10.52	Br
52425.405	14.48	13.48	12.18	10.73	Be	52483.379	14.28	13.08	11.89	10.57	Be
52425.464	-	13.59	-	-	VM	52484.389	-	13.15	-	-	VM
52427.354	14.57	13.65	-	10.74	Vy	52484.393	14.23	13.24	12.03	10.55	Vy
52427.440	-	13.48	12.13	10.75	On	52485.334	14.34	13.23	12.02	10.54	Vy
52429.352	-	13.49	12.12	10.68	Br	52485.371	-	13.15	-	-	VM
52429.433	-	13.57	-	-	VM	52485.373	14.35	13.07	11.86	10.54	Be
52430.408	14.45	13.48	12.15	10.72	Be	52487.347	14.41	13.17	12.04	10.55	Vy
52430.433	-	13.49	12.10	10.73	On	52487.419	-	13.13	-	-	VM
52430.451	-	13.57	-	-	VM	52488.365	-	13.16	-	-	VM
52437.423	14.47	13.36	12.06	10.66	Be	52488.373	13.81	13.14	11.98	10.54	Vy
52438.389	-	13.43	12.08	10.62	Br	52490.350	14.27	13.16	12.02	10.54	Vy
52438.466	-	13.47	-	-	VM	52490.377	14.23	13.04	11.83	10.55	Be
52440.396	-	13.41	-	-	VM	52490.427	-	13.18	-	-	VM
52443.305	14.58	13.37	12.15	10.64	At	52492.328	14.24	13.19	12.02	10.53	Vy
52443.373	-	13.30	12.01	10.61	Br	52492.405	-	13.16	-	-	VM
52443.434	-	13.37	-	-	VM	52497.400	-	13.10	-	-	VM
52444.409	14.46	13.22	12.00	10.64	Be	52504.341	14.21	12.98	11.78	10.52	Be
52444.447	-	13.35	-	-	VM	52506.326	-	12.96	11.72	10.45	Br
52445.298	14.57	13.34	12.14	10.61	At	52509.267	14.26	13.28	11.86	10.48	At
52445.383	-	13.32	-	-	VM	52513.342	-	13.07	-	-	VM
52446.294	-	13.45	12.13	10.61	At	52516.316	-	13.09	-	-	VM
52446.381	-	13.31	-	-	VM	52517.302	-	13.09	-	-	VM
52446.411	14.46	13.33	-	10.65	Vy	52517.306	-	12.97	11.75	10.45	Br
52448.349	14.73	13.31	-	10.63	Vy	52520.332	-	13.12	-	-	VM
52448.392	-	13.31	-	-	VM	52521.379	-	13.12	-	-	VM
52449.397	-	13.30	-	-	VM	52522.315	-	13.12	-	-	VM
52450.354	-	13.28	11.99	10.61	Br	52523.398	-	13.07	11.79	10.60	On
52451.394	-	13.34	-	-	VM	52525.302	-	13.10	-	-	VM
52452.406	-	13.35	-	-	VM	52525.304	14.20	13.04	11.81	10.53	Be
52453.344	-	13.23	12.00	10.60	Br	52525.373	-	13.03	11.78	10.55	On
52453.378	-	13.37	-	-	VM	52526.290	-	13.11	-	-	VM
52454.300	14.56	13.32	12.14	10.62	At	52526.361	-	13.01	11.78	10.52	On
52454.348	-	13.29	11.99	10.59	Br	52526.472	-	13.12	11.77	10.50	At
52454.419	14.52	13.37	12.14	10.64	Vy	52528.315	-	13.10	-	-	VM
52455.309	14.54	13.38	12.14	10.62	At	52530.292	-	13.10	-	-	VM
52455.387	14.67	13.40	12.14	10.64	Vy	52530.349	-	13.00	11.77	10.52	On
52455.470	-	13.37	-	-	VM	52534.246	14.25	13.07	11.92	10.51	At
52456.422	14.42	13.39	12.15	10.65	Vy	52536.240	14.17	13.09	11.92	10.51	At
52457.313	14.53	13.36	12.15	10.63	At	52537.315	-	13.04	-	-	VM
52457.365	14.83	13.41	12.15	10.71	Vy	52544.233	14.26	12.98	11.86	10.48	At

Table 1. Photometry of YY Her in the B, V, R and I filters - continued

MJD	B	V	R	I	Ob	MJD	B	V	R	I	Ob
52547.261	14.13	12.88	11.73	10.49	Be	52767.438	-	12.57	-	-	VM
52547.276	-	12.99	-	-	VM	52784.454	-	12.60	11.38	10.49	On
52548.260	-	12.99	-	-	VM	52789.438	-	12.61	11.40	10.49	On
52548.260	-	12.93	11.74	10.44	Br	52790.462	-	12.60	11.39	10.48	On
52557.205	14.24	13.00	11.86	10.48	At	52793.356	-	12.70	11.38	10.44	Br
52566.288	14.05	12.85	11.76	10.45	At	52793.451	-	12.62	11.37	10.45	On
52573.193	14.18	12.89	11.72	10.43	At	52794.539	-	12.59	11.43	10.49	On
52574.227	-	12.80	11.61	10.40	Br	52795.500	-	12.61	11.41	10.48	On
52590.186	14.09	12.81	11.73	10.44	At	52798.540	-	12.65	11.39	10.48	On
52591.172	14.04	12.88	11.74	10.47	At	52799.393	-	12.69	11.41	10.45	Br
52596.194	-	12.82	11.66	10.44	Br	52807.462	-	12.63	11.39	-	On
52619.192	-	12.73	-	-	VM	52808.446	-	12.60	11.38	10.46	On
52661.697	-	12.80	-	-	VM	52818.393	-	12.71	11.38	-	VM
52670.699	-	12.83	-	-	VM	52819.389	-	12.73	11.39	-	VM
52672.681	13.68	12.69	11.56	10.47	Be	52823.427	-	12.59	11.41	10.41	On
52682.645	13.54	12.63	11.50	10.48	Be	52836.439	-	12.64	11.42	10.44	On
52693.629	12.18	11.70	11.00	10.27	Be	52840.442	-	12.59	11.42	10.42	On
52694.700	-	11.75	-	-	VM	52841.387	-	12.69	11.36	-	VM
52695.700	-	11.75	-	-	VM	52842.440	-	12.63	-	-	VM
52696.500	-	11.72	-	-	VM	52844.350	-	12.62	11.37	-	VM
52696.654	12.18	11.75	-	-	SL	52845.459	-	-	11.35	-	VM
52697.600	-	11.81	-	-	VM	52847.459	-	12.66	11.37	-	VM
52697.648	12.29	11.83	-	-	SL	52848.459	-	12.64	11.38	-	VM
52698.642	12.26	11.85	-	-	SL	52853.410	-	12.62	11.36	-	VM
52703.600	-	11.93	-	-	VM	52862.438	-	12.70	11.43	-	VM
52703.626	12.43	11.87	11.03	10.30	Be	52863.440	-	12.72	11.43	-	VM
52703.630	12.41	11.95	-	-	SL	52864.426	-	12.71	11.40	-	VM
52705.591	12.48	11.97	-	-	SL	52867.381	-	12.70	11.36	-	VM
52706.600	-	11.98	-	-	VM	52877.322	-	12.66	11.40	-	VM
52712.700	-	12.03	-	-	VM	52888.335	-	12.76	11.49	-	VM
52715.600	-	12.02	-	-	VM	52900.365	-	-	11.52	-	VM
52715.619	-	12.00	11.06	10.27	Br	52901.374	-	12.83	11.55	-	VM
52720.500	-	12.23	-	-	VM	52905.366	-	12.89	11.57	-	VM
52720.570	12.93	12.12	11.19	10.40	Be	52908.321	-	12.89	11.60	-	VM
52720.594	-	12.23	11.20	10.37	Br	52919.306	-	-	11.64	-	VM
52721.500	-	12.22	-	-	VM	52925.318	-	13.00	11.70	-	VM
52721.545	-	12.17	11.19	10.37	On	52931.358	-	13.09	11.75	-	VM
52722.528	12.88	12.19	11.21	10.36	Be	52944.226	-	13.17	11.86	-	VM
52723.500	-	12.25	-	-	VM	52946.255	-	-	11.92	-	VM
52723.527	-	12.20	11.19	10.35	On	52948.248	-	13.31	11.92	-	VM
52724.600	-	12.29	-	-	VM	52949.295	-	13.30	11.94	-	VM
52726.600	-	12.29	-	-	VM	52950.237	-	13.30	11.92	-	VM
52730.568	-	12.15	-	-	VM	52957.219	-	13.38	11.96	-	VM
52734.525	-	-	11.08	10.33	Be	52964.199	-	13.45	11.98	-	VM
52745.472	13.01	12.17	11.10	10.31	Be	52965.208	-	13.45	11.98	-	VM
52745.497	-	12.24	-	-	VM	52966.206	-	13.40	11.98	-	VM
52746.474	-	12.26	-	-	VM	52967.202	-	-	11.96	-	VM
52749.472	13.08	12.28	11.14	10.36	Be	52968.194	-	13.44	-	-	VM
52749.518	-	12.30	-	-	VM	52971.193	-	13.54	-	-	VM
52750.473	13.08	12.27	11.16	10.37	Be	52976.204	-	13.52	12.03	-	VM
52750.489	-	12.33	-	-	VM	52977.210	-	13.58	12.07	-	VM
52751.487	-	12.35	-	-	VM	52978.207	-	13.51	12.02	-	VM
52754.455	-	12.35	-	-	VM	52981.196	-	13.54	12.09	-	VM
52761.448	13.29	12.57	-	-	SL	52983.186	-	13.55	12.10	-	VM
52763.432	13.32	12.49	11.28	10.43	Be	52984.219	-	13.49	12.02	-	VM
52763.456	-	12.53	-	-	VM	52993.177	-	13.45	12.03	-	VM
52764.476	-	12.54	-	-	VM	52996.186	-	13.47	12.01	-	VM
52766.739	-	12.56	-	-	VM						

light curves, the transformations towards the previous published data used were found (see. thereinbefore). The final shifts for the individual observatories and the individual filters are listed in Table 2. The typical error of the individual shifts is in the range of (0.02–0.03) mag.

Table 2. The conversion table of the zero-points of the individual observatories

Observatory	Shifts in Filter			
	B	V	R	I
Athens (At)	0.13	0.11	-0.36	-0.52
Beluša (Be)	0.23	0.23	-0.23	-0.56
Brno (Br)	0.66	0.17	-0.22	-0.51
Kryonerion (Kr)	0.23	0.11	-	-
Ondřejov (On)	-	0.23	-0.20	-0.56
St. Lesná (SL)	0.22	0.12	-	-
Val. Meziříčí (VM)	-	0.11	-0.18	-
Vyškov (Vy)	0.23	0.11	-0.37	-0.56

These homogenised data are shown in Fig. 1. The contributions from the individual observatories are distinguished by means of the special symbols. The historical light curve in the V band depicted in Fig. 2 is constructed from our campaign data (filled circles) as well as the data from the literature (triangles). Two main outbursts, which occurred in May 1993 and February 2003, are clearly visible in this figure. The light curve of YY Her obtained only at one observatory (Be) was published by Hric *et. al* (2001 a) in their Fig. 1. Detected on the light curve are the non-linear decline of the brightness from the previous outburst, two primary minima and the depth of the brightness between two primary minima. The discovered depth was interpreted by us for the first time as the secondary minimum. The data obtained during our international campaign (see Fig. 1) really confirmed the presence of the secondary minimum on the basis of independent observations from many participating observatories. The light curves in the individual filters are covered very well with a relatively small scatter except for the B pass-band where the light curve is considerably noisy with a deformed shape of the minima. This is connected with the facts that the brightness of the object in the B filter is low and therefore near the limit of a majority of the equipments used. Moreover, the quantum efficiency of the used CCD detectors is reduced in this spectral region.

The secondary minimum is clearly visible in all filters, while the depth of the minimum becomes smaller towards the longer wavelengths. The brightness of the object declined by 0.6, 0.5, 0.4 and 0.35 mag in the B, V, R and I filter, respectively. The shape of the secondary minimum is moderately asymmetric, while the decline to the minimum is sharper than the increase from the minimum. According to the ephemeris, published in the work by Hric *et al.* (2001 a),

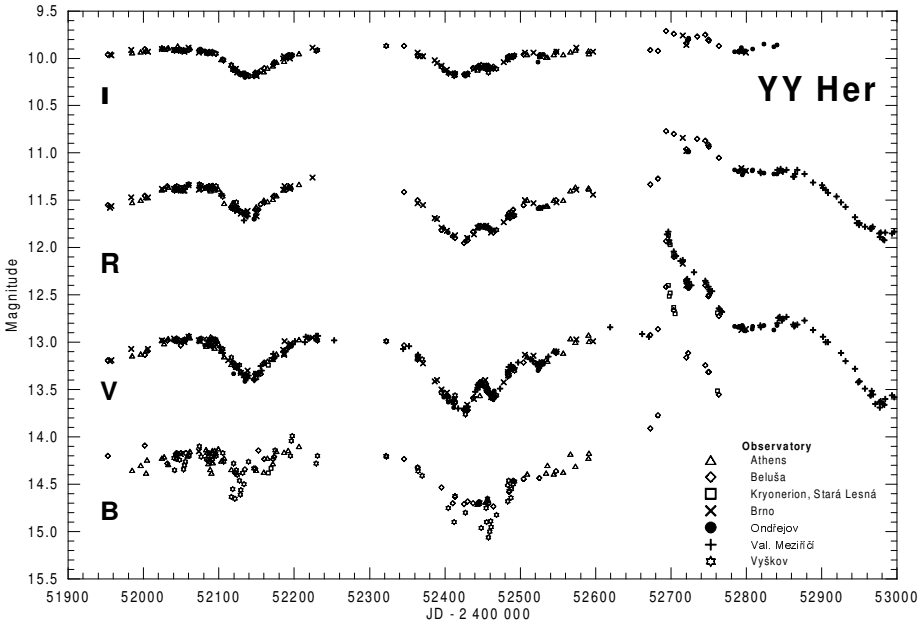

Figure 1. *BVRI* photometry of YY Her secured during the international campaign from 2001 to 2003.

the time of the secondary minimum occurred in the orbital phase of 0.45, which indicates that the orbit could be elliptical. However, this is very unlikely because all of over 20 symbiotic stars with known spectroscopic elements and with orbital periods below 1000 days have circular orbits. A more plausible explanation of this observational fact will be mentioned in the next section. The observational sets are interrupted due to a seasonal gap in winter 2001/2002. In the following observing season, all observatories were integrated again to the monitoring of the object and the achieved results were unique. The primary minimum, observed in most detail up to now, was unexpectedly deformed by two flares. The shape of the minimum is asymmetric and, in addition, the moment of the minimum of the light curve does not fit the moment of the minimum predicted according to the above-mentioned ephemeris. The brightness began to increase about a month before the expected moment of the primary minimum and reached the first maximum in JD 2 452 450. The next maximum was reached in less than 40 days. The decline of the brightness between these two maxima synchronises with the time of the primary minimum computed according to the ephemeris given by Hric *et al.* (2001 a). It looks like that this activity predicted also the main outburst that occurred around JD 2 452 700. The maximum of the brightness of the outburst was reached very quickly after the rise of the

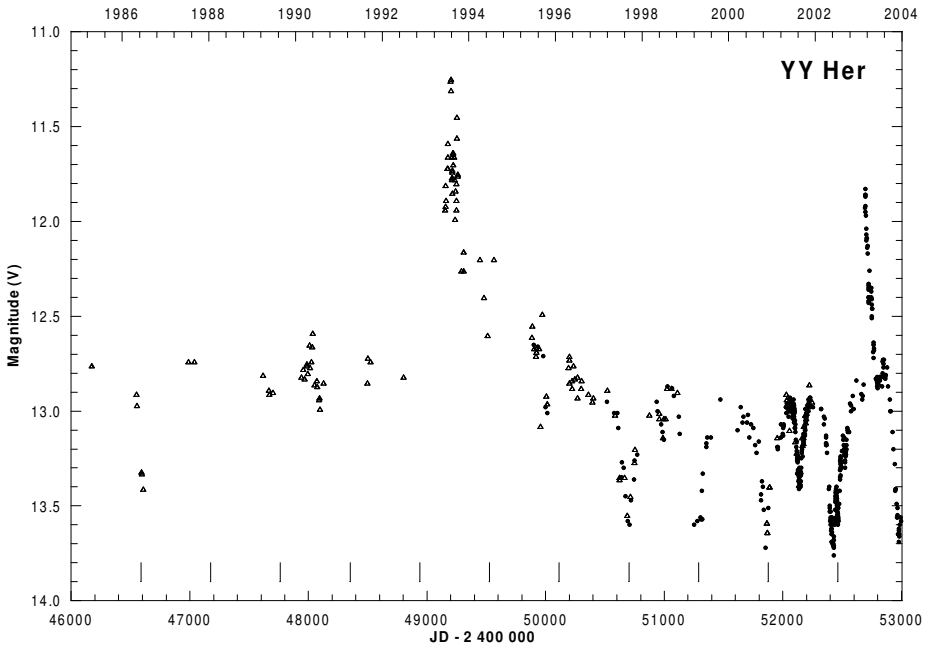

Figure 2. The V light curve of YY Her covering the period 1986-2004. The campaign data are depicted by filled circles and the data from the literature are marked by triangles. The times of minima calculated according to our ephemeris (Hric *et al.* 2001 a) are depicted by vertical dashes. This historical light curve shows only recent history of the YY Her light behaviour. The most pronounced activity of the light curve is a large outburst that appeared in 1993. The light curve was covered insufficiently and inhomogeneously before this outburst. Nevertheless, the shape of the curve allows us to suspect the existence of one primary minimum in 1986 and one secondary minimum in 1990. Both minima match well our new eclipsing model of the system.

event (15 days) and the decline to the pre-outburst level was finished 107 days after the maximum. It is evident that the amplitude of the outburst declines towards longer wavelengths. For a given pass-band, the following amplitudes at maximum were detected: 1.56, 1.04, 0.54 and 0.20 mag in the B, V, R and I filter, respectively. The monotonous decline of brightness from the maximum was interrupted by an apparent dip that is in good agreement with the time of the secondary minimum. Both secondary minima (JD 2 452 145 and JD 2 452 730) occurred in phase of 0.45 according to our ephemeris (Hric *et al.*, 2001 a) in spite of that the second one occurred during the main outburst. It is very strong evidence that the secondary minima are due to geometrical eclipses. The study of outburst activity, energies and durations of observed events will be the subject of our next paper.

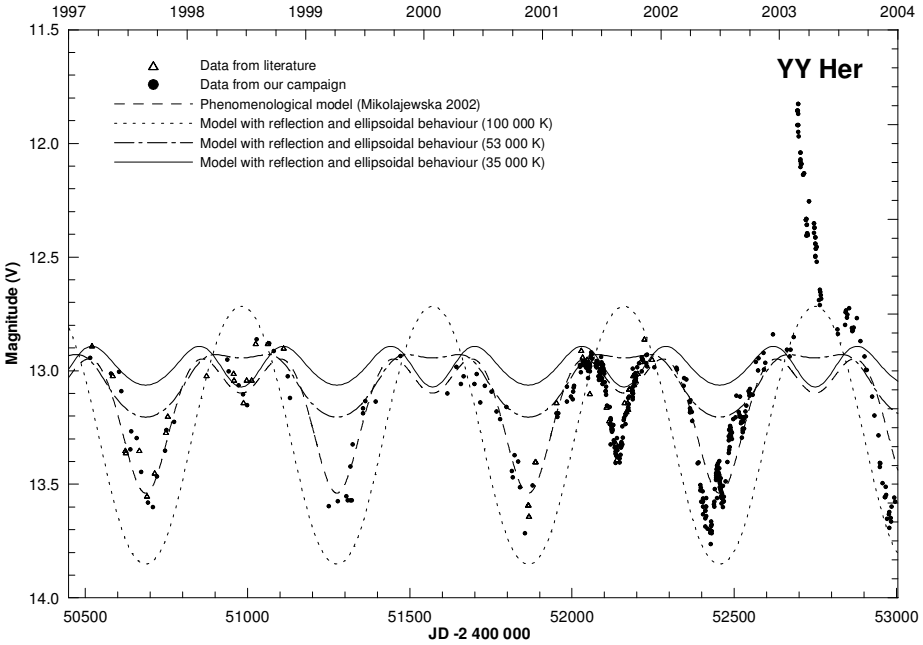

Figure 3. The V light curve of YY Her with particular models. The dashed line represents the phenomenological model with parameters presented by Mikolajewska (2002) which is combination of variable nebular emission and ellipsoidal changes of the red giant. The dotted line, dot-and-dashed line and solid line represent the physical models with reflection and ellipsoidal behaviour with the $T_{\rm WD}$ = 100 000 K, 53 000 K and 35 000 K, respectively.

4. The eclipsing model

Mikolajewska *et al.* (2002) proposed the phenomenological model to explain the existence of the secondary minimum of YY Her in which the periodic changes can be described by a combination of the ellipsoidal effect and sinusoidal variations of the nebular continuum and line emission. Unfortunately, the data used in their analysis had a very large scatter. Our new data revealed the shape of the secondary minimum as well as that of the primary minima with a high accuracy. The first inspection of the light curves of YY Her casts doubts on the model by Mikolajewska *et al.* (2002). Both minima have well defined beginnings and ends and the brightness between the minima changes only slightly. It is also worth noting that in order to describe such light curves it is necessary to take the higher harmonic members (> 2) into account, but such an interpretation would be problematic. Nevertheless, we constructed the model curves

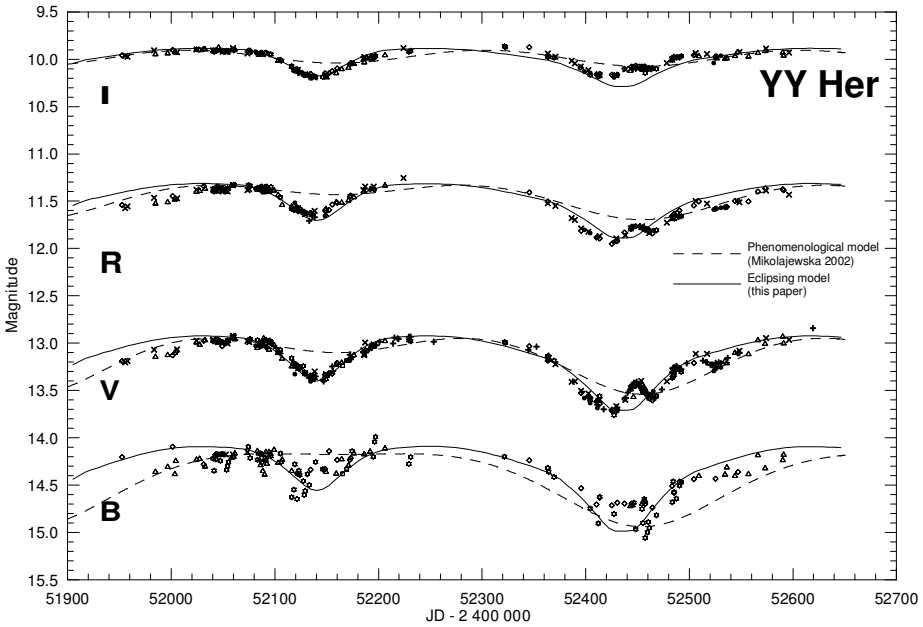

Figure 4. The B, V, R and I light curves of YY Her covering one orbital cycle. The dashed line represents the phenomenological model with parameters presented by Mikolajewska (2002). The solid line represents our best fit of the eclipsing model.

in particular colours with parameters listed in Table 3 in paper published by Mikolajewska *et al.*(2002). These curves are depicted by dashed lines in Figs. 3 and 4. It is clear that this phenomenological model does not fit the new B, V, R and I photometric observational data, mainly the shape and the depth of the secondary minima.

We tested the interpretation by means of the reflection and ellipsoidal effects using the code assigned to light curve analysis of binaries – Binary Maker 2.0 (Bradstreet, 1993). We assumed a simplified binary model: the white dwarf (WD)and the cool giant (c) at or near its Roche lobe. The obtained results are shown in Fig. 3. The starting parameters were set as follows: $T_{\rm WD} = 100\,000$ K, $T_{\rm c} = 3500$ K, $q = M_{\rm c}/M_{\rm WD} = 2$. In this case, the reflection effect was so pronounced that the ellipsoidal effect was suppressed, one minimum was absent and the light curve had a sinusoidal shape (doted line in Fig. 3). Because the white dwarf can be embedded in a circumstellar nebula that dramatically changes its radiating characteristics, we decreased the temperature of the white dwarf during the next steps and traced the changes of the synthetic light curves. The second minimum appeared for the temperature $T_{\rm WD} < 53\,000$ K (dot-and-dashed line in Fig. 3). For $T_{\rm WD} \approx 35\,000$ K (solid line in Fig. 3.), both minima

had the same depth and for the lower temperatures the secondary minimum was deeper than the primary one. For any combination of input parameters, the synthetic light curves did not respond to the observed light variations either by the shape or by the depth of the minima in the individual pass-bands.

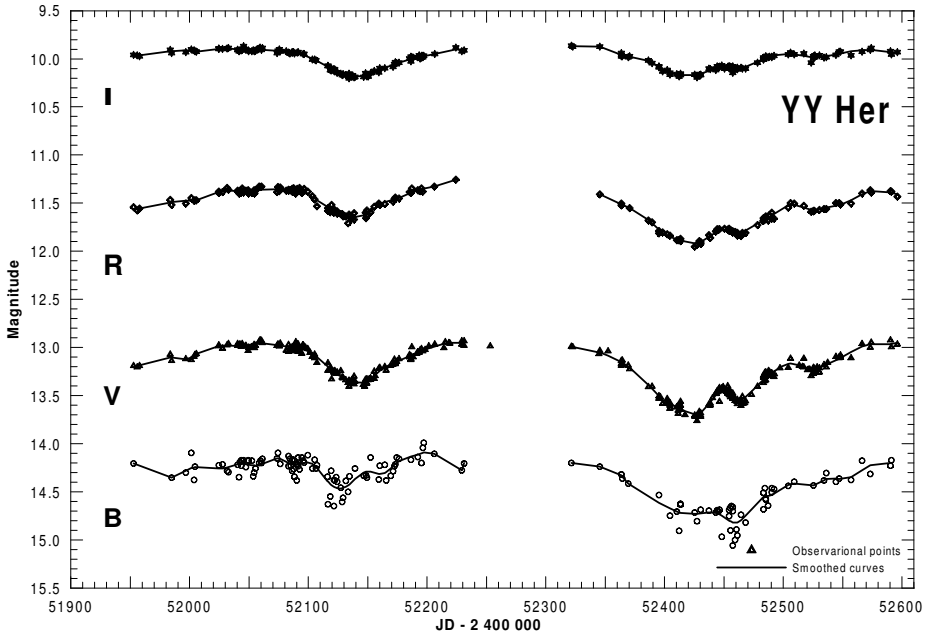

Figure 5. The observed points in the B, V, R and I filters are depicted by open circles, triangles, diamonds and asterisks, respectively, together with the smoothed curves marked by solid lines.

In the next step, we attempted to explain the observed light variations by the eclipsing model (Fig. 4). The size of the white dwarf in any case is not sufficient to produce the minima of the observed duration. As mentioned above, it is probable that the white dwarf is embedded in an expanding envelope (Huang, 1984). If this circumstellar material is optically thick the envelope is able to eclipse the red giant. In such a case, the envelope can be described by the model of stellar atmosphere. The white dwarf was substituted by a normal star and the parameters of the system were optimised to fit the observed light curves by the synthetic ones. The result of this optimisation process is the model with the red giant near to its Roche lobe and the white dwarf embedded in the envelope (en) with the temperature $T_{\rm en} = 4000$ K. The envelope lies inside its Roche

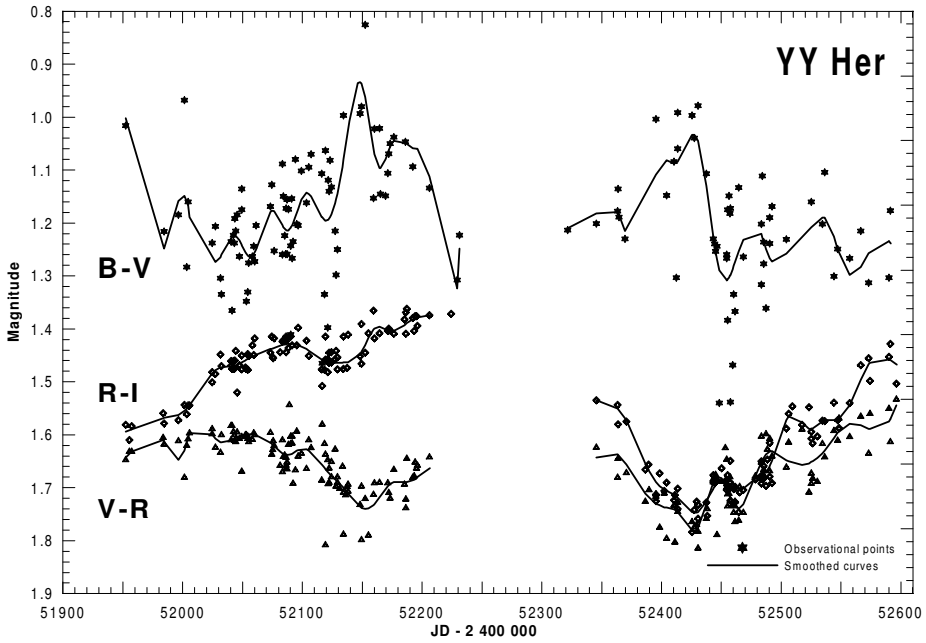

Figure 6. The smoothed curves of the colour indices (solid lines) together with the original data.

lobe. The eclipses of the red giant and the envelope occur during the orbital cycle because the inclination of the orbital plane is $i \approx 85°$.

The course of the light curve of YY Her can enable us to derive the radius of the envelope around the accretor. As the duration of the secondary minimum we determined the value of 96 days. We have adopted the radius of the giant $R_{\rm g} = 110R_{\odot}$ as well as the radius of the circular orbit $A_{\rm circ} = 403R_{\odot}$ by Skopal (2005). Afterwards the radius of the envelope is $R_{\rm en} = 100R_{\odot}$ for inclination of $i = 85°$. The values of the radius and the temperature, derived in the previous item lead to the envelope luminosity $L_{\rm en} = 2290L_{\odot}$, which corresponds to absolute bolometric magnitude $M_{\rm en(bol)} = -3.65\,$mag. Using the bolometric correction $BC_{\rm en} = -0.88\,$mag by Lang (2002) we can derive the absolute magnitude of the envelope in V colour $M(V)_{\rm en} = -2.77\,$mag and afterwards the apparent magnitude $m(V)_{\rm en} = 11.22\,$mag for the distance of the object $d = 6.3\,$kpc (Skopal, 2005). The observed apparent magnitude in the secondary minimum is $m(V)_{\rm en} = 13.38\,$mag. If we take into account the interstellar reddening for $E_{\rm (B-V)} = 0.2\,$mag (Skopal, 2005) we get the corrected apparent magnitude $m(V)_{\rm en} = 12.66\,$mag. This magnitude is by 1.44 mag less than the value computed on the base of the luminosity of the envelope. The possible ex-

planation of this difference is in a disk-like structure of the envelope around the white dwarf.

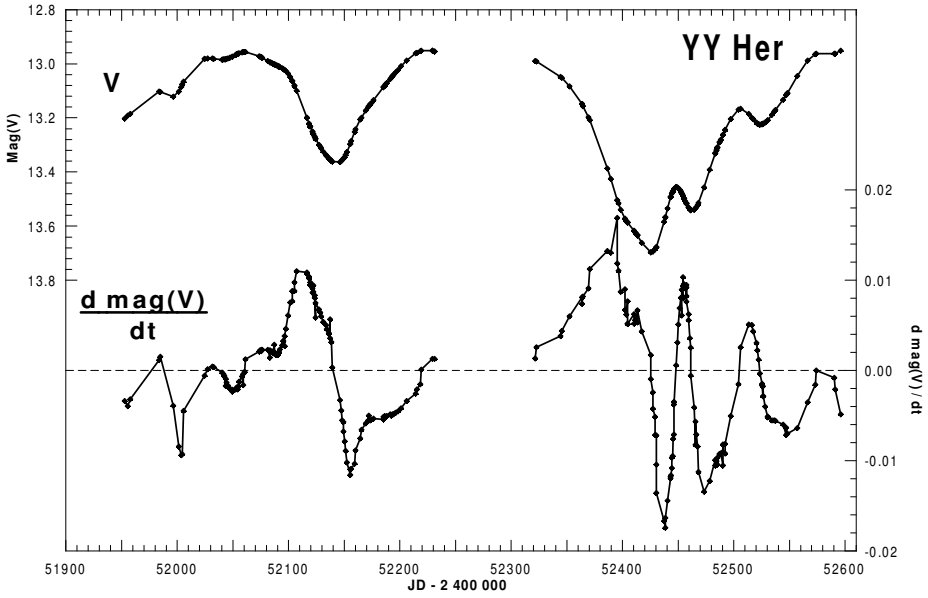

Figure 7. The light curve of the secondary and primary minima from the smoothed data (top) and the derivation of this smoothed light curve (d mag(V)/dt) in the V filter (bottom).

5. Analysis of the colour indices

The light curves of YY Her in the individual filters were smoothed by the code HEC13 (author: Dr. Harmanec, method: Vondrák 1969, 1977). This code can fit (only in a mathematical frame) a smooth curve to the data no matter what their course is. This code calculates one "smoothed" point to each observed point. It makes use of two input parameters, ϵ and ΔT. ϵ determines how "tight" the curve will be, that is if just the main course or also the high-frequency variations are to be reproduced. ΔT is the interval over which the data are binned before smoothing. The individual observations in the $BVRI$ filters together with the smoothed curves are shown in Fig. 5. The smoothing yielded very good results for the curves in the V, R, I filters inside the densely covered interval of JD 2 451 950 – 2 452 600, but it was slightly less reliable for the B band light curve due to a larger noise in the data. The colour index was then determined

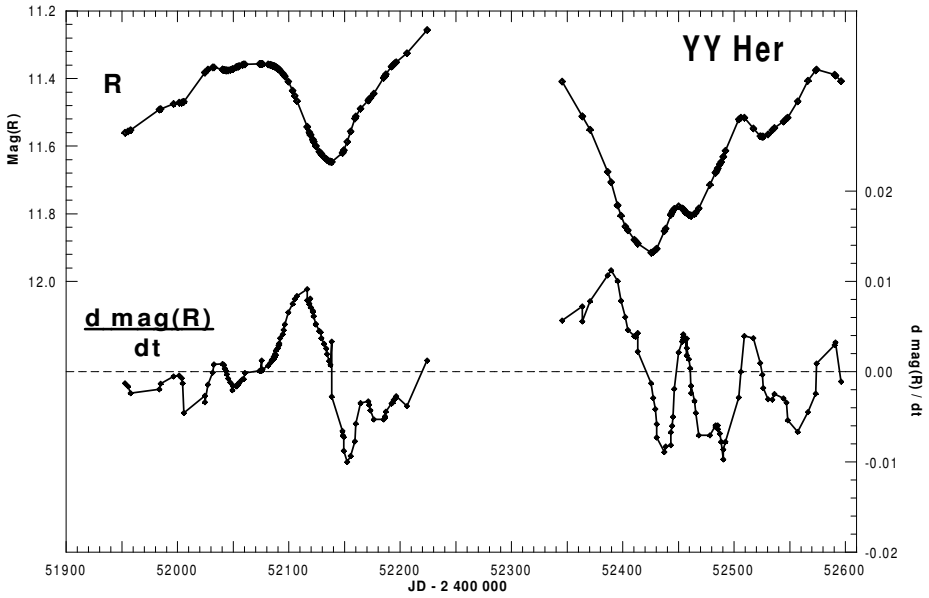

Figure 8. The light curve of the secondary and primary minima from the smoothed data (top) and the derivation of this smoothed light curve (d mag(R)/dt) in the R filter (bottom).

from the difference between the individual fitted curves in the individual filters, not directly from the observed data. This approach resulted in the curves of the colour indices with a much smaller noise and with more subtle details apparent. These fitted curves of the colour indices together with the original indices are shown in Fig. 6. The following notes consider only the densely covered interval of JD 2 451 950 – 2 452 600 (one primary and one secondary minimum).

The temporal course of the indices $V-R$, $R-I$, $B-V$:

– $V-R$: An almost identical depth (the value of $V-R$) in the primary and secondary minimum is obvious. $V-R$ reddens with the decreasing brightness in both minima.

– $R-I$: The index reddens in both minima (prim. and sec.) but the reddening of $R-I$ is much larger in the primary minimum than in the secondary one. A prominent trend of a long-term decrease of $R-I$ is apparent between JD 2 451 950 and JD 2 452 210. A reddening of $R-I$ in the secondary minimum is superimposed on this trend. The beginning of the secondary minimum in this index is very clearly visible, a fact which is in favour of a real secondary eclipse in YY Her. The largest reddening of the $R-I$ and

$V-R$ indices (at about JD 2 452 430) occurred before the real primary minimum (at about JD 2 452 460).

– $B-V$: A larger noise and, hence, some small artefacts occurred during fitting but a pronounced decrease of $B-V$ in the secondary minimum is real. Approximately the same decrease of $B-V$ in about JD 2 452 430 (before the primary minimum!) as well as a possible small reddening of $B-V$ in the real primary minimum is observed.

The waves in the profiles of the colour indices in the rising branch of the eclipse are present in the secondary eclipse and the courses of $V-R$ and $R-I$ indices are in good agreement with each other. The waves in the rising branch of the light curve of the primary minimum are apparent in the V, R and I filter. The decreases of brightness in the "waves" lead to a reddening in both the $V-R$ and $R-I$ indices (most prominent near JD 2 452 525).

A striking asymmetry of the profile of the secondary minimum, visible in the V and R filters, was emphasised by a derivation of the fitted light curve in the V and R filters (Figs. 7 and 8). The maximum rate of change of mag(V) (d mag(V)/dt) is the same for the descending and ascending branch of the eclipse but the upper part of the ascending branch is considerably slower and longer than the descending branch (this is true also for the R filter). The derivation of the fitted light curve was applied also to the profile of the primary minimum and the preceding dip.

The course of the colour indices can enable us to constrain the region radiating mainly in the B filter. This region is just slightly (partially) eclipsed in the secondary minimum while it is largely eclipsed in the primary one. During the dip that occurred before the primary minimum the region is only slightly (partially) eclipsed. The colours of the dip differ considerably from the colours of the primary minimum. A possible physical interpretation is that the region, which radiates in B is more vertically extended than the matter radiating in VRI. This region lies in the vicinity of the white dwarf and maybe surrounds it. The dip (JD 2 452 425) prior to the time of the primary minimum could be caused by a vertically extended region (spray) where the mass stream from the cool donor star impacts on the disk around the white dwarf. This spray (if optically thick) can occult a part of the (outer) disk projected behind this spray. This event is not unusual because the similar behaviour is detected in X-ray binaries, not in optical, but in X-ray region. The large decrease of $B-V$ at this moment can suggest that the inner disk region is just partially occulted (maybe due to a relatively low inclination of the orbital plane or due to a larger vertical extension of the matter radiating in B).

6. Discussion

The photometric behaviour of YY Her suggests the presence of the optically thick envelope (see section 4). Such envelope would result characteristic spectroscopic appearance that is actually observed. Spectra of YY Her are characterised by very strong nebular emission. The emission spectrum rich in Fe II lines was observed during the outburst. The high-ionization lines of He II were also present (Tatarnikova *et al.* 2000, 2001). The emission lines ratios are consistent with a model with a nebula photo-ionised by a hot and luminous companion, probably a white dwarf. If this white dwarf is embedded in an optically thick and extended envelope (to produce measurable eclipses of the red giant), one should not observe the strong high ionisation emission lines in optical and UV spectra. It seems that the envelope is inhomogeneous as suggested also by the determination of envelope luminosity (see section 4) as well as by the variations of the colour indices and the derivation of the light curves (see section 5). The fact that the both observed secondary minima occurred in phase 0.45 can suggest that the envelope is asymmetric against joint of the binary components on circular orbit. The opaque part of envelope around the white dwarf can have a shape of a thick disc with a vertically extended rim or toroid than is optically thick in direction of orbital plane and its size is sufficient to produce observed eclipses of the secondary component. This envelope can be optically thin in the vertical line and thus the circumstellar matter above and below the orbital plane can be photo-ionised and to generate the observed emission spectral lines. This matter is accelerated by radiation pressure and a bipolar structure of outflows or sprays can be created. If these outflows are oblique (not perpendicular) to the line of sight they should produce two components of particular emission line profiles with opposite mean radial velocities. This model is supported by spectroscopic observations by Huang (1984). He showed that emission Balmer lines are separated into two components by a deep blue-shifted reversal. Presence of expanding circumstellar matter is also suggested by the He I (5876, 7065) lines which exhibit distinct P Cyg profiles. The centers of the absorption components are shifted from the emission ones by $v_{\rm r} \approx 100\,{\rm km\,s^{-1}}$, suggesting moderate outflow velocities (Tatarnikova *et al.* 2001).

7. Conclusion

The results of a long-term photometric monitoring of symbiotic binary YY Her is possible to summarise as follows:

– The light curve is not possible to explain by the phenomenological model by Mikolajewska *et al.* (2002.

– The light behaviour is possible to explain by eclipses of the red giant and presence of an opaque envelope around the white dwarf.

– The light curve analysis revealed the temperature of the envelope around the white dwarf of 4000 K.

– The estimation of envelope luminosity suggests that it is not spherically symmetric, but a thick torus shape or disc. This explanation requires the presence of an inhomogeneous and optically thick (in direction of orbital plane) envelope around the white dwarf.

– The model of a disk-like structure envelope is supported by a colour indices analysis as well as by the presence of strong emission lines in the spectrum of the object.

– The photometric observations show the existence of the unexpected activity (flare interrupted by eclipse of an active region around the white dwarf) followed by the main outburst.

The analysis of activity of the symbiotic star YY Her will be the subject of our next paper. High resolution spectroscopic data are inevitable for determination of the nature of YY Her.

Acknowledgements. We are indebted to Dr. Harmanec for providing us the code HEC13. This work was supported by the VEGA grant 4015/4.

References

Allen, D.A.: 1979, in *IAU Coll. 46, Changing Trends in Variable Stars Research*, eds.: F. Bateson , J. Smak and I. Urch, Univ. of Waikato, New Zealand, 1

Blair, W., Stencel, R.E., Feibelman, W.A.,Michalitsianos, A.G.: 1983, *Astrophys. J., Suppl. Ser.* **53**, 573

Böhme, S.: 1938, *Astron. Nachr.* **268**, 73

Bradstreet, D.H.: 1993, *Binary Maker 2.0 User Manual*, Contact Software, Norristown

Herbig, G.H.: 1950, *Publ. Astron. Soc. Pac.* **62**, 211

Hric, L., Petrík, K., Niarchos, P, Velič Z., Gális, R.: 2001a, *Inf. Bull. Variable Stars* **5046**, 1

Hric, L., Petrík, K., Velič, Z., Gális, R.: 2001 b, *Perseus* **1**, 4

Hric, L., Skopal, A.: 1989, *Inf. Bull. Variable Stars* **3364**, 1

Huang, C.C.: 1984, *Astron. Astrophys.* **135**, 410

Kenyon, S.J., Webbing, R.F.: 1984, *Astrophys. J.* **279**, 252

Lang, K.R.: 1992, *Astrophysical Data, Planets and Stars*, Springer-Verlag, New York

Michalitsianos, A.G., Kafatos, M., Feibelman, W.A., Hobbs, R.W.: 1982, *Astrophys. J.* **253**, 735

Mikolajewska, J., Kolotilov, E.A., Shugarov, S. Yu, Yudin, B.F.: 2002, *Astron. Astrophys.* **392**, 197

Munari, U., Kolotilov, E.A., Popova, A.A., Yudin, B.F.: 1997 a, *Astron. Zh.* **74**, 898

Munari, U., Rejkuba, M., Hazen, M., Mattei, J., Schweitzer, E., Luthardt, R., Shugarov, S., Yudin, B.F., Popova, A.A., Chugainov, P.V., Sostero, G., Lepardo, A.: 1997 b, *Astron. Astrophys.* **323**, 113

Mürset, U., Nussbaumer, H., Schmid, H.M., Vogel, M.: 1991, *Astron. Astrophys.* **248**, 458
Nussbaumer, H., Schild, H., Schmid, H.M., Vogel, M.: 1988, *Astron. Astrophys.* **198**, 179
Plaut, L.: 1932, *Astron. Nachr.* **244**, 296
Skopal, A.: 2005, *Astron. Astrophys.* **440**, 995
Tatarnikova, A.A., Esipov, V.F., Kolotilov, E.A., Mikolajewska, J., Munari, U., Shugarov, S. Yu.: 2001, *Astronomy Letters* **27**, No. 11, 703
Tatarnikova, A.A., Rejkuba, M., Buson, L.M., Kolotilov, E.A., Munari, U., Yudin, B.F.: 2000, *Astron. Zh.* **77**, 220
Vondrák, J.: 1969, *Bull. Astron. Inst. Czechosl.* **20**, 349
Vondrák, J.: 1977, *Bull. Astron. Inst. Czechosl.* **28**, 84
Waagen, E.O.: 2003, *IAU Circ.* **8083**, 1
Wolf, M.: 1919, *Astron. Nachr.* **208**, 147